Measurements of the THz absorption and dispersion of ZnTe and their relevance to the electro-optic detection of THz radiation

G. Gallot, Jiangquan Zhang, R. W. McGowan, Tae-In Jeon, and D. Grischkowsky
School of Electrical and Computer Engineering and Center for Laser and Photonic Research, Oklahoma State University, Stillwater, Oklahoma 74078

(Received 22 February 1999; accepted for publication 14 April 1999)

Via THz time-domain spectroscopy, we have measured the absorption and index of refraction of single-crystal ⟨110⟩ ZnTe from 0.3 to 4.5 THz. We find that the absorption is dominated by two lower-frequency phonon lines at 1.6 and 3.7 THz and not by the transverse-optical (TO) -phonon line at 5.3 THz as previously assumed. However, the index of refraction is determined mainly by the TO-phonon line. Using these data, we discuss a frequency-domain picture of electro-optic detection of THz radiation below the TO-phonon resonance and compare with the photoconductive THz receiver over the same frequency range. © *1999 American Institute of Physics.* [S0003-6951(99)03523-8]

The application of optoelectronic techniques to the generation and detection of THz electromagnetic radiation is now well established. These techniques have enabled the widely practiced method of THz time-domain spectroscopy (THz-TDS),[1] demonstrations of THz imaging,[2,3] and THz ranging.[4] The two primary optoelectronic methods for the detection of THz radiation are photoconductive antenna and electro-optic sampling. Although electro-optic (EO) THz receivers have demonstrated exceptionally high-frequency performance,[5] they have not demonstrated the continuous spectral coverage of photoconductive receivers, due to the strong THz absorption and dispersion of the EO crystal, phase mismatch between the interrogating light pulse and the propagating THz pulse, and a strong frequency dependence of the EO susceptibility. The comparison of photoconductive receivers with EO receivers is of significant interest and experimental comparisons have been performed.[6,7]

Although ZnTe has been the primary EO detection crystal,[3,5–10] and even though detailed simulations have been compared with experimental results,[10] the frequency-dependent absorption and dispersion of ZnTe have not been previously measured to the best of our knowledge. Here, via THz-TDS, we present measurements of the index of refraction and absorption of ZnTe from low frequencies to 4.5 THz. In contrast to what has been previously assumed, we find that the absorption below 4.5 THz is not dominated by the strong transverse-optical (TO) -phonon line at 5.3 THz, but instead the measured absorption shows several new phonon lines. In fact, below 3.5 THz we do not observe significant absorption from the low-frequency wing of the TO-phonon line. However, as previously expected, the behavior of the index of refraction is dominated by the TO-phonon resonance.

We have recently presented a complete frequency-domain description of electro-optic detection of pulsed THz electromagnetic radiation, which shows the effect of EO detection as the product of three spectral filters (described in detail later in this letter) acting on the complex amplitude spectrum of the incoming THz pulse.[11] Given our characterization data for ZnTe, we can now apply this frequency-domain picture of EO detection in order to gain an understanding of the limits of EO detection with ZnTe below the TO-phonon resonance at 5.3 THz.

Our THz-TDS measurements of the absorption and index of refraction of a series of ZnTe crystals with different thicknesses are presented in Fig. 1 together with the spectral response of the THz-TDS system. As can be seen in Fig. 1(a), the amplitude spectrum of a single measurement of the THz reference pulse with no sample in place is quite clean with excellent signal-to-noise ratio (S/N) and good dynamic range. The amplitude frequency response of the THz photoconductive receiver employed is to a good approximation given by the square root of this spectrum, which is indicated by the upper dashed line in Fig. 1(a).[12] We used several 10 mm×10 mm ZnTe crystals of lengths of 0.997, 0.192, and 0.120 mm to obtain our results, depending on the strength of the absorption at the frequency range under investigation. The crystals are ⟨110⟩ cut and were obtained from II–VI, Inc. The most difficult data to obtain were the highest-frequency measurements made with the 120 μm thick crystal optically contacted to a high-resistivity Si plate. For these data we averaged 64 individual measurements of both the reference and signal pulses to obtain increased S/N to enable our measurements to 4.5 THz. The resulting power absorption coefficient shown in Fig. 1(b) has several surprises. First, the absorption of the wing of the strong TO-phonon line only becomes a significant part of the observed absorption for frequencies above 3.5 THz. Second, there is a broad resonance line centered at 1.6 THz with a peak power absorption coefficient of 13 cm^{-1} and another much stronger broad feature centered at 3.7 THz with a peak absorption of approximately 90 cm^{-1}. These powerful features overwhelm the weaker effect of the absorption from the wing of the 5.3 THz line, as indicated by the solid line giving the self-consistent calculated absorption of the TO-phonon line. These features are due to longitudinal and transverse-acoustic (TA) phonon absorption lines, which have been previously indirectly observed by spectroscopy in the far infrared,[13] and by Raman scattering.[14] The results are both in quite good agreement with the observed lines, enabling us to

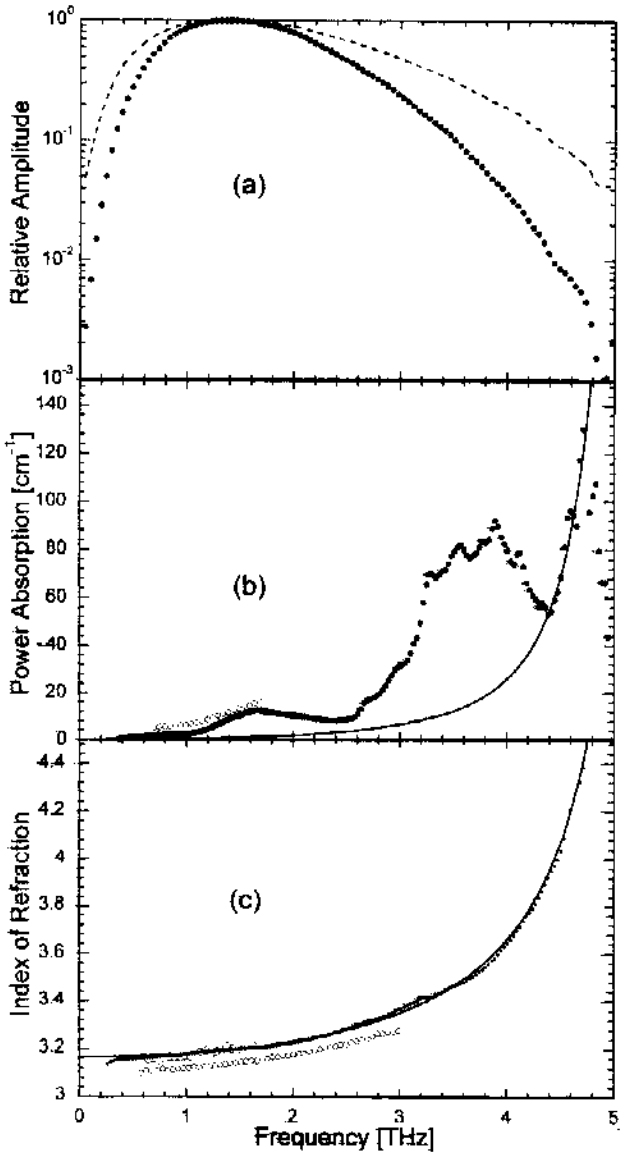

FIG. 1. (a) Measured amplitude spectrum (dots) of the reference THz pulse with no ZnTe sample in place. The dashed line indicates the amplitude frequency response of the photoconductive THz receiver (Ref. 12). (b) Our measured (dots) power absorption coefficient (cm^{-1}) for ZnTe crystal compared with the calculated (solid line) absorption for the TO-phonon line. The upper curve indicated by the open circles from 0.6 to 1.7 THz is a previous measurement (Ref. 16). (c) Our measured (dots) index of refraction of ZnTe crystal compared to the calculated index (solid line) for the TO-phonon line. Previous measurements (Ref. 16) at room temperature (large open circles) and helium temperature (small open circles, lower curve from 0.5 to 3 THz) are also indicated.

assign the line at 1.6 THz to the transverse TA(X) phonon, and the line at 3.7 THz to the longitudinal LA(X) phonon. The open circles show a previous measurement from 0.6 to 1.7 THz (upper curve).[16]

The power absorption spectrum shown in Fig. 1(b), which is self-consistent for all our crystals, strongly affects EO detection with ZnTe. In fact, due to the absorption of the strong line at 3.7 THz, for crystal thicknesses greater than 0.5 mm the frequency response of EO detection on the low side of the TO-phonon resonance extends to only 3 THz. These results show the technical risk of extrapolating EO crystal performance, based only on the knowledge of the TO-phonon frequency. For example, GaAs has a TO-phonon frequency of 8.0 THz, but shows significant measured absorption in the frequency range from 0.2 to 5 THz.[1,15] In contrast to the absorption results, the index of refraction measurements shown in Fig. 1(c) are clearly dominated by the strong TO-phonon line. Here, we have observed a dramatic increase in the index as the resonance is approached. As expected, the effect of the strong absorption line at 3.7 THz is also seen on these index data. For comparison we show the previous measurements at both room (large open circles) and helium temperatures (small open circles).[16] Our comparative results dramatically demonstrate the efficacy of THz-TDS for such characterizations. These excellent results for the index characterization when compared with the solid line theoretical fit show that the resonant frequency is more accurately 5.32 THz and enable us to determine the other parameters of the TO-phonon resonance as shown below.

Using the dielectric response of a harmonic oscillator of the form[10]

$$\epsilon(\Omega)=\epsilon_{el}+\frac{\epsilon_{st}\Omega_{TO}^2}{\Omega_{TO}^2-\Omega^2+2i\gamma\Omega}=(n+i\kappa)^2, \tag{1}$$

where $\epsilon(\Omega)$ is the frequency-dependent dielectric constant and ϵ_{st} describes the strength of the TO-phonon resonance at $\Omega_{TO}/2\pi$. We fit our measured index of refraction n with the parameters $\Omega_{TO}/2\pi=5.32$ THz, $\epsilon_{el}=7.44$, $\epsilon_{st}=2.58$, and the linewidth of the resonance $\gamma/2\pi\leq 0.025$ THz. This measured upper limit for the linewidth is less than 1/6 the previously assumed value.[10] The power absorption coefficient $\alpha=4\pi\kappa/\lambda_0$, is determined by κ, where λ_0 is the free-space wavelength. These values can be compared to those of Ref. 16 with no damping, for which $\Omega_{TO}/2\pi=5.4$ THz, $\epsilon_{el}+\epsilon_{st}=9.92$, and $\epsilon_{el}=6.0$. Clearly, as indicated by the comparison in Fig. 1(c), our measurements have the ability to define these parameters more precisely than the previous work. It is noteworthy that the index of refraction data accurately determine Ω_{TO}, ϵ_{el}, and ϵ_{st}, but are relatively insensitive to the linewidth γ. In contrast, the absorption data are very sensitive to the parameter γ. In our case the small contribution by the TO-phonon line to the total observable absorption sets an upper limit on γ, which is much narrower than previously assumed.[10]

Insight into THz EO measurements with ZnTe is gained by incorporating these precise measurements of the index and absorption into the theoretical calculation for the EO signal. As described in the frequency domain, the EO signal is given by[11]

$$S(\tau)\propto\int_{-\infty}^{+\infty}A_{THz}(\Omega)f(\Omega)e^{-i\Omega\tau}d\Omega, \tag{2}$$

where

$$f(\Omega)=C_{opt}(\Omega)\chi_{eff}^{(2)}(\omega_0;\Omega,\omega_0-\Omega)\left[\frac{e^{i\Delta k_+(\omega_0,\Omega)l}-1}{i\Delta k_+(\omega_0,\Omega)}\right]. \tag{3}$$

This result expresses the time-dependent EO signal $S(\tau)$ as a relatively simple Fourier integral over the THz angular frequency range Ω, which is easily evaluated. $f(\Omega)$ is the product of three frequency-dependent terms that act as spectral filters on the incoming THz complex spectral amplitude $A_{THz}(\Omega)$. If $f(\Omega)$ would have a smooth spectral response much broader than $A_{THz}(\Omega)$, the measured EO signal would

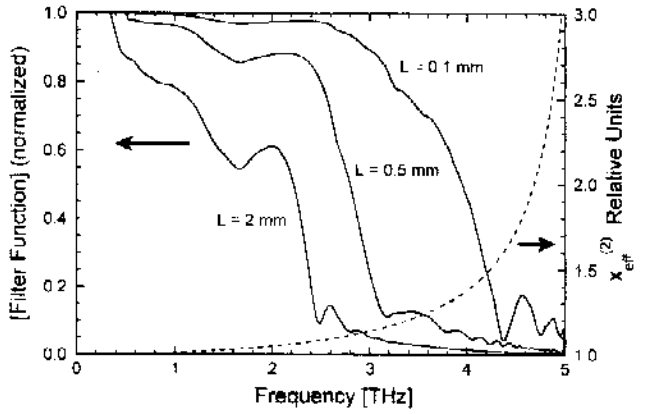

FIG. 2. Calculated $\chi^{(2)}_{\text{eff}}$ (dashed line) shown on a relative scale (right ordinate). Calculated and normalized to the unity (left ordinate) filter function in the brackets in Eq. (3) shown as the solid lines, using the measured absorption and index of refraction for ZnTe and the indicated crystal thicknesses of $l=0.1$ mm, $l=0.5$ mm, and $l=2$ mm.

be essentially the same as the THz pulse entering the EO crystal. However, usually this is not the case. For the terms that comprise $f(\Omega)$ in Eq. (3), ω_0 is the carrier frequency of the optical probing pulse, and l is the crystal length. Referring to Ref. 11 for the propagation vector mismatch $\Delta k_+ = -k(\omega_0+\Omega)+k(\Omega)+k(\omega_0)$, which is to an excellent approximation[9] given by $\Delta k_+ \approx k(\Omega)-\Omega/v_g$, where v_g is the optical group velocity. The first filter $C_{\text{opt}}(\Omega)$ is the complex spectrum of the autocorrelation of the probing light pulse. Typically, the optical bandwidth $\Delta\omega$ is much larger than the THz bandwidth so that this term has little effect. The second filter describes the EO susceptibility $\chi^{(2)}_{\text{eff}}$, which can be strongly frequency dependent, and can thereby distort the EO signal and the corresponding spectrum, independent of the thickness of the EO crystal.[11] The third filter describes the frequency-dependent coherence length determined by the mismatch between the optical probing pulse traveling at the optical group velocity and the frequency components of the THz pulse propagating at their respective phase velocities determined by the frequency-dependent index of refraction. The third filter term enclosed by the brackets, reduces to the well-known parametric result, $l\,\text{sinc}(\Delta k_+ l/2)$ for real Δk_+, while the imaginary part of Δk_+ describes the usually strong absorption of the THz radiation by the EO crystal. The effect of this term is reduced by making the EO crystal thickness l as small as possible. In the limit of very small thickness, Eq. (2) is similar to the result obtained by Auston and Nuss.[17] The combined effect of all these terms can severely distort the EO signal, and reduce and cause discontinuities in the corresponding measured THz spectrum.

The relatively dramatic frequency dependence of $\chi^{(2)}_{\text{eff}}$ crossing over the TO-phonon resonance has been presented from 0 to 15 THz in Ref. 11. Here, in Fig. 2 we show (dashed line) the frequency dependence of $\chi^{(2)}_{\text{eff}}$ from low frequencies to 5 THz. For this range, $\chi^{(2)}_{\text{eff}}$ increases monotonically with frequency by more than three times as the TO-phonon resonance is approached. Given the index of refraction and absorption data of Fig. 1, and $\Delta k_+(\omega_0,\Omega)$, we can evaluate the filter function in the brackets in Eq. (3). Figure 2 shows (solid lines) the calculated absolute value of this filter function in the brackets for the crystal lengths of 0.1, 0.5, and 2 mm. In order to normalize all three curves to unity, they have each been divided by their corresponding crystal length. Although increasing the crystal length will increase the detection sensitivity, increasing the length will also increase the effects of phase mismatch and absorption, which in turn reduces the effective bandwidth of the EO detection process. In order to compare these EO frequency-domain results with the corresponding frequency response of the photoconductive receiver, these curves can be compared with the dashed line in Fig. 1(a). In summary, from this analysis of EO detection with ZnTe below the TO-phonon resonance, the useful frequency range is significantly limited by the crystal properties. In comparison, the photoconductive receiver can cover this frequency range below the TO-phonon resonance with a smooth spectral response.

The authors acknowledge careful readings of this manuscript and the many helpful and stimulating suggestions by R. Alan Cheville. This work was partially supported by the National Science Foundation and the U.S. Army Research Office.

[1] D. Grischkowsky, S. Keiding, M. van Exter, and Ch. Fattinger, J. Opt. Soc. Am. B **7**, 2006 (1990).
[2] D. M. Mittleman, R. H. Jacobsen, and M. C. Nuss, IEEE J. Sel. Top. Quantum Electron. **2**, 679 (1996).
[3] Q. Wu, T. D. Hewitt, and X.-C. Zhang, Appl. Phys. Lett. **69**, 1026 (1996).
[4] R. A. Cheville, R. W. McGowan, and D. Grischkowsky, IEEE Trans. Antennas Propag. **45**, 1518 (1997).
[5] Q. Wu and X.-C. Zhang, Appl. Phys. Lett. **71**, 1285 (1997).
[6] Y. Cai, I. Brener, J. Lopata, J. Wynn, L. Pfeiffer, J. B. Stark, Q. Wu, X.-C. Zhang, and J. F. Federici, Appl. Phys. Lett. **73**, 444 (1998).
[7] S.-G. Park, M. R. Melloch, and A. M. Weiner, Appl. Phys. Lett. **73**, 3184 (1998).
[8] Q. Wu and X.-C. Zhang, Appl. Phys. Lett. **68**, 1604 (1996).
[9] A. Nahata, A. S. Weling, and T. F. Heinz, Appl. Phys. Lett. **69**, 2321 (1996).
[10] H. J. Bakker, G. C. Cho, H. Kurz, Q. Wu, and X.-C. Zhang, J. Opt. Soc. Am. B **15**, 1795 (1998).
[11] G. Gallot and D. Grischkowsky, J. Opt. Soc. Am. B (to be published).
[12] N. Katzenellenbogen, H. Chan and D. Grischkowsky, in OSA Proceedings on Ultrafast Electronics and Optoelectronics, Vol. 14, Proceedings of the Topical Meeting 25–27 January, 1993, San Francisco, California, pp. 123–125.
[13] R. E. Nahory and H. Y. Fan, Phys. Rev. **156**, 825 (1967).
[14] J. C. Irwin and J. Lacombe, J. Appl. Phys. **41**, 1444 (1970).
[15] S. E. Ralph and D. Grischkowsky, Appl. Phys. Lett. **60**, 1070 (1992).
[16] T. Hattori, Y. Homma, A. Mitsuishi, and M. Tacke, Opt. Commun. **7**, 229 (1973).
[17] D. H. Auston and M. C. Nuss, IEEE J. Quantum Electron. **24**, 184 (1988).